Yasir, Ahmed T. ; Hawari, Alaa H. ; Talhami, Mohamed ; Baune, M. ; Thöming, Jorg ; Du, Fei

The impact of electric field on the demulsification efficiency in an electro-coalescence process

Recommended Citation (primary publication/Version of Record) incl. DOI:

Ahmed T. Yasir, Alaa H. Hawari, Mohammed Talhami, M. Baune, J. Thöming, Fei Du,
The impact of electric field on the demulsification efficiency in an electro-coalescence process,
Journal of Electrostatics, Volume 122, 2023, 103796, ISSN 0304-3886,
https://doi.org/10.1016/j.elstat.2023.103796.

Take down policy
If you believe that this document or any material on this site infringes copyright, please contact
publizieren@suub.uni-bremen.de with full details and we will remove access to the material.

The impact of electric field on the demulsification efficiency in an electro-coalescence process

Ahmed T. Yasir[a], Alaa H. Hawari[a,*], Mohammed Talhami[a], M. Baune[b], J. Thöming[b] and Fei Du[b]

[a] Department of Civil and Architectural Engineering, Qatar University, P.O. Box 2713, Doha, Qatar.

[b] Center for Environmental Research and Sustainable Technology, University of Bremen, Leobener Str. 6, D 28359 Bremen, Germany.

*Corresponding author: Dr. Alaa H. Hawari; Tel.: +(974) 3393-1555; Fax: +(974) 4403-4172.

E-mail address: a.hawari@qu.edu.qa

Abstract

In this study, the influence of the electric field and its determining parameters such as voltage, inter-electrode distance and frequency on the demulsification efficiency of a water-in-oil emulsion was studied. The numerical analysis showed that the water droplets trapped onto the hydrophobic titanium dioxide (TiO_2) coated electrodes and at 2 mm inter-electrode distance can increase the electric field intensity above 300 kV/m, where droplet rupture takes place. Experimental study showed highest demulsification efficiency of 76% while applying AC voltage of 250 V, frequency of 200 kHz and inter-electrode distance of 4 mm.

Keywords: Water-in-oil emulsion; Dielectrophoresis; Demulsification; High frequency alternating current.

1. Introduction

Naturally, crude oil contains large amount of dispersed water droplets with an average radius of 50 μm. Turbulent mixing, agitation through downhole wellbore, surface chokes and other drilling activities disperse these water droplets and emulsifies the droplets in the oil system [1]. Crude oil also contains other substances such as asphaltenes, resins, naphthenic acids and other solid particles [2, 3]. These natural surfactants prevent the rupture of the water droplets hence stabilizes the emulsion by preventing coalesce of the water droplets in crude oil [4]. The existence of these water droplets in oil results in corrosion of the pipeline and reduces the efficiency of the pumps and heat exchangers [1, 5]. In the industry, demulsification of water-in-oil emulsion is carried out by adding chemical demulsifiers such as poly alkylene oxides, poly alkylene glycol, ethylene oxide, polyamines, fatty alcohols, alkyl phenols, fatty acid ester and mercaptans [6]. These chemicals are expensive and can create toxic byproducts, thus, better demulsification processes are still being investigated. The primary aim of the demulsification process is to coalesce the water drops which then can be easily separated by gravity. To promote droplet coalescence, Romanova et al. (2022) injected aluminum nitride (AlN) suspended in acetone as an additive in the emulsion and ultrasonicated the emulsion [7]. In the process, by adding 8 v/v% additive, 99% demulsification was achieved within 3 min of ultrasonication. Cao et al. (2022) modified a polyacrylonitrile (PAN) microfiltration membrane with polytetrafluoroethylene (PTFE) nanofiber to demulsify a water-in-oil emulsion [8]. In this study, the membrane casted with 9% PTFE achieved 99.99% demulsification efficiency along with a permeate flux of 4,909 LMH. Zhu et al. (2022) coated a recycled wet wipe with hydrogel and carried out demulsification of an oil/water emulsion stabilized by cationic surfactants [9]. During demulsification, the negatively charged hydrogel surface attracted the positively charged surfactants which promoted demulsification. The process achieved <99% demulsification efficiency with a flux of 3,057 LMH. Apart from chemical demulsifiers, the coalescence of water droplets can also be promoted by

59   adding biological demulsifiers, thermal treatment, membrane demulsification, electrical

60   demulsification and microwave irradiation [10]. Among the different technologies used for the

61   demulsification of water-in-oil emulsions, the electrical demulsification technology is considered

62   as one of the simplest, the most environmentally friendly and the most efficient technology with

63   lowest energy demand [11, 12]. In electrical demulsification, a uniform or non-uniform electric field

64   is applied to polarize the water droplets. The net charge on water droplets induces electrophoretic

65   (EP) force in a uniform electric field. The polarization of water droplets generates dielectrophoretic

66   force (DEP) in a non-uniform electric field. The presence of EP or DEP in the system promotes

67   coagulation of the water droplets. The main challenges for an electrical demulsification process

68   include formation of pearl chain, electrochemical reactions on the electrode surface and formation

69   of secondary droplets. To avoid formation of pearl chains, high frequency non-uniform AC electric

70   field has been suggested by Zhou et al. (2022) [13]. Mousavi et al. (2014) carried out

71   demulsification of a water-in-oil emulsion using poly(methyl methacrylate) coated polished brass

72   electrodes and applied a pulsatile electric field (PEF) [14]. In the study, by applying PEF at 100

73   Hz to a sunflower oil-based emulsion, coalescence was achieved without the formation of

74   secondary droplets. The study also found that by applying direct current (DC) in sawtooth

75   waveform is better for prevention of secondary droplet formation than applying DC with square or

76   half-sinusoidal waveform. Less et al. (2008) studied demulsification of water-in-oil emulsion using

77   the Aibel Vessel Internal Electrostatic Coalescer (VIEC) where the electrodes were insulated with

78   an epoxy coating [15]. In the study, applying an alternating current (AC) at high voltage with the

79   addition of 20 ppm chemical demulsifier resulted in the removal of 95% water from the emulsion

80   within 5 mins, whereas, without applying an alternating current only 80% water was removed from

81   the emulsion. Li et al. (2022) studied the electrocoalescence process of water droplets in

82   sunflower oil in a non-uniform electric field and in laminar flow conditions using different electrode

83   arrays [16]. The numerical study showed that higher electric field intensity can be achieved in the

84   electrocoalescence process by using the mesh electrode array compared to the grid electrode

85 array. Moreover, the study also found that, at high Reynold's number, the demulsification

86 efficiency increases. Table 1 summarizes the mechanisms, advantages and disadvantages of the

87 different demulsification techniques.

88 In this work, for a better and deeper understanding of the electrocoalescence process, we

89 numerically simulated and experimentally demonstrated the influence of electric field on the

90 demulsification efficiency by varying the electric field determining parameters (including voltage,

91 frequency and distance between electrodes). In addition, the impact of the entrapment of water

92 droplets on the surface of the electrodes was investigated. An optimal design of an

93 electrocoalescence process to achieve high demulsification efficiency with low energy demand

94 was suggested.

95 **Table 1.** Summary of different demulsification technologies with their advantages and disadvantages.

Demulsification technique	Mechanism	Advantages	Disadvantages	References
Chemical demulsification	Chemical demulsifiers are amphiphilic in nature and reduces the surface tension of the emulsion by adsorbing oil and water on its surface. The reduction of surface tension promotes coalescence of the water droplets.	-Simple operation -Low residence time -Cost effective	-High toxicity -Non-renewable	[17]
Biological demulsification	In biological demulsification, bacteria is used to reduce the interfacial tension which in turn promote coalescence of the droplets.	-Low toxicity -Biodegradable -High efficiency at extreme conditions	-Vulnerable to sudden operation changes	[18]
Thermal demulsification	In thermal demulsification, application of heat reduces the viscosity of oil and water. This reduces the mechanism strength of the interfacial films and increases mobility of the particles. These promotes coalescence of the water droplets.	-Dissolves paraffin crystals -No harmful byproducts	-Loss of light oil fraction -Lower separation efficiency -Increased corrosion risk	[19]
Membrane demulsification	In this process, a membrane is used to separate the oil/water droplets from the bulk solution.	-Free of chemical contaminants -Low energy requirement	-Concentration polarization	[8]

			-Difficult to regenerate membranes	
Electrical demulsification	In this process, electric field is used to cause collision among the water droplets which in turn will promote droplet coalescence.	-Environment friendly -Lower energy consumption	-Formation of secondary droplet	[20]
Microwave irradiation	In this process, by using microwaves, the molecules of the components in the dispersed phase are rotated which increases ionic conduction of the particles. The increased ionic conduction promotes coalescence of the particles.	-Low treatment time -Selective heating of the dispersed phase -No chemical contaminants	-Low separation efficiency	[21]

96

7

2. Methodology

2.1 Preparation of the water-in-oil emulsion

QALCO performance oil #68 was utilized to prepare the water-in-oil emulsion. Table 2 summarizes the properties of the used oil. The total volume of the water-in-oil emulsion used during all the studies was 100 ml. The water content in the emulsion was varied between 2.51-11.27 wt%. The oil and water were dispersed using an Ultra Turrax T25 (IKA) disperser in a 500 mL beaker. The disperser can operate at a dispersion speed between 3,000 and 25,000 rpm. The oil and water mix were dispersed for 5 to 20 minutes. The concentration of water in the water-oil emulsion was measured using a moisture analyzer (OHAUS, Germany). The moisture analyzer works by heating the sample to 120 °C to evaporate all the available water in the emulsion. The difference in weight before and after evaporation indicates the moisture content of the emulsion.

Table 2. Properties of the oil used for preparing the water-in-oil emulsion.

Flash Point	220°C
Appearance	Clear Amber Yellow
Physical State	Liquid
Vapor Density (air=1)	>1
Boiling Point	>260 °C
Solubility in Water	Negligible
Specific Gravity	0.875
Viscosity	42-50 cSt
Conductivity	<0.001 µS/cm

110   To find the lowest water content, samples were taken from different locations of the sample holder

111   and it showed a gradual decrease in water content along the depth of the sample holder where

112   the lowest water content was found at the top and the highest water content was found at the

113   bottom. The stability of the water-in-oil emulsion was evaluated by examining the water

114   concentration on the surface of the water-in-oil emulsions prepared under different conditions,

115   such as mixing speed, dispersion time, and water content in the emulsion. Under these conditions,

116   water content was plotted as a function of time. To identify emulsion stability, the slope of the

117   points was determined. Higher stability was indicated by lower slope.

118   The effect of water content on the stability of the water-in-oil emulsion was studied by varying the

119   water content between 2.51 and 11.27 wt% at a constant dispersion speed of 10,000 RPM and 5

120   minutes of dispersion time. As shown in **Figure S1** of the Supplementary Information, higher

121   water content in the emulsion reduced the stability of the prepared emulsion. This is because, at

122   higher water concentrations, the number of water droplets in the emulsion is higher. This presents

123   more opportunity for the water droplets to collide, coalesce and form larger droplets which then

124   settle easily by gravity and reduce the stability of the emulsion. Since the demulsification

125   experiments will be carried out for 60 mins, and the stability of the emulsion for both 2.51 wt%

126   and 4.71 wt% water-in-oil emulsion is almost similar with slopes of -0.0004 and -0.0005,

127   respectively, a water content of 4.71 wt% was used to prepare the emulsions. Using 4.71 wt%

128   water and 5 minutes of dispersion time, the effect of dispersion speed on the stability of the water-

129   in-oil emulsion was studied. As presented in **Figure S2** of the Supplementary Information, a

130   dispersion speed of 5,000 RPM gave the lowest stable emulsion presented by the highest slope

131   of its tendency line. Whereas dispersion speed of 10,000 RPM and higher gave almost the same

132   stability of the emulsion. Therefore, in this study, dispersion speed of 10,000 RPM was used to

133   prepare the water-in-oil emulsion. At 10,000 RPM dispersion speed and 4.71 wt% water content,

134   the effect of dispersion time on the stability of the water-in-oil emulsion was studied. As shown in

Figure S3 of the Supplementary Information, a dispersion time of 5 minutes presented the highest stable water-in-oil emulsion where the difference of water content of the emulsion after 180 minutes was only 0.24 wt%. The very unstable emulsion after longer dispersion times is mainly due to the heat generated by the high-speed mixer. It was noticed that at 10,000 RPM the temperature of the emulsion increased from 23°C at 5 minutes dispersion time to 42°C after 20 minutes of dispersion time (**Figure S4** of Supplementary Information). The increased temperature promotes coalescence of the water droplets which reduces stability of the emulsion. It can be also noticed from **Figure S2** and **Figure S3** that, although the initial water concentration for the dispersion speed and dispersion time study was fixed at 4.71 wt%, after dispersion, the initial water content was not identical. This is because, while using the homogenizer, mechanical heating was induced in the system as indicated by **Figure S4**. Thus, at higher dispersion time and dispersion speed water was lost from the system as indicated by lower initial water content at higher dispersion time and speed. This was also a factor for deciding the optimum dispersion time and speed. The selected dispersion time of 5 mins and dispersion speed of 10,000 RPM showed lowest loss of water due to mechanical heating. Hence, we considered the emulsion to be more stable while using these operating conditions.

The water droplet size analysis was carried out using a MALVERN Zetasizer nano (UK) and can be seen in **Figure S5** of the Supplementary Information. As seen in **Figure S5**, increasing the water content in the emulsion also resulted in increased water droplet size in the emulsion. The largest and smallest average water droplet size in the prepared water-in-oil (W/O) emulsion was found to be 797 nm and 291 nm for W/O emulsion with 11.27 wt% and 2.51 wt% water, respectively. Generally, the presence of bigger water droplets makes the emulsion less table, whereas smaller water droplet size would result in higher emulsion stability.

158   2.2 Experimental setup

159   The experimental setup for the demulsification process comprised of a high-frequency AC power

160   supply (G 2000, Redline Technologies), an oscilloscope (MDO3024, Tektronix) utilized to

161   measure the current (A) and the voltage (U), two titanium electrodes, and a glass vial (length: 10

162   cm, diameter: 15 mm). The titanium electrodes were 2 mm in diameter. The electrodes surface

163   was coated with a 200 nm thin film insulating layer of hydrophobic titanium oxide (TiO_2, rutile).

164   The electrodes were coated with TiO_2 hydrophobic layer in order to reduce the electrowetting

165   effect and the high-pass filter effect. In addition, the TiO_2 coating will eliminate electrochemical

166   reactions on the surface of the electrodes, prevent the formation of gas bubbles, and corrosion of

167   the electrodes.

168   Figure **1** (a) shows a schematic diagram of the experimental set up. During the demulsification

169   process, 10 mL of the stable water-in-oil emulsion was placed in the glass vial and a high

170   frequency AC voltage was supplied by the AC power supply where the waveform of the current

171   and voltage measured by the oscilloscope was a Sine wave. The water content at the top of the

172   emulsion was analyzed after 15, 30, 45 and 60 minutes of demulsification. The demulsification

173   performance using high frequency AC was compared with low frequency AC and direct current

174   (DC). All experiments were repeated three times and the average of the results is reported.

175   Moreover, the standard deviation of the results is expressed in the form of error bars. The

176   demulsification efficiency (η_w), represented by the efficiency of water removal, was calculated as:

$$\eta_w = \frac{C_{wt} - C_{w0}}{C_{w0}} \tag{1}$$

177

178   where, C_{w0} is water content at the beginning of the experiment (wt%), C_{wt} is the water content at

179   the end of demulsification process (wt%). To observe the formation of the water droplets, a 3D

180   printed module with channels for electrodes and water-in-oil emulsion was designed (

181   Figure **1** (b)). The 3D printed module was equipped with an industrial machine vision camera

182   (MER-112-32U3C, Daheng Imaging) connected to a computer for data collection and analysis.

183
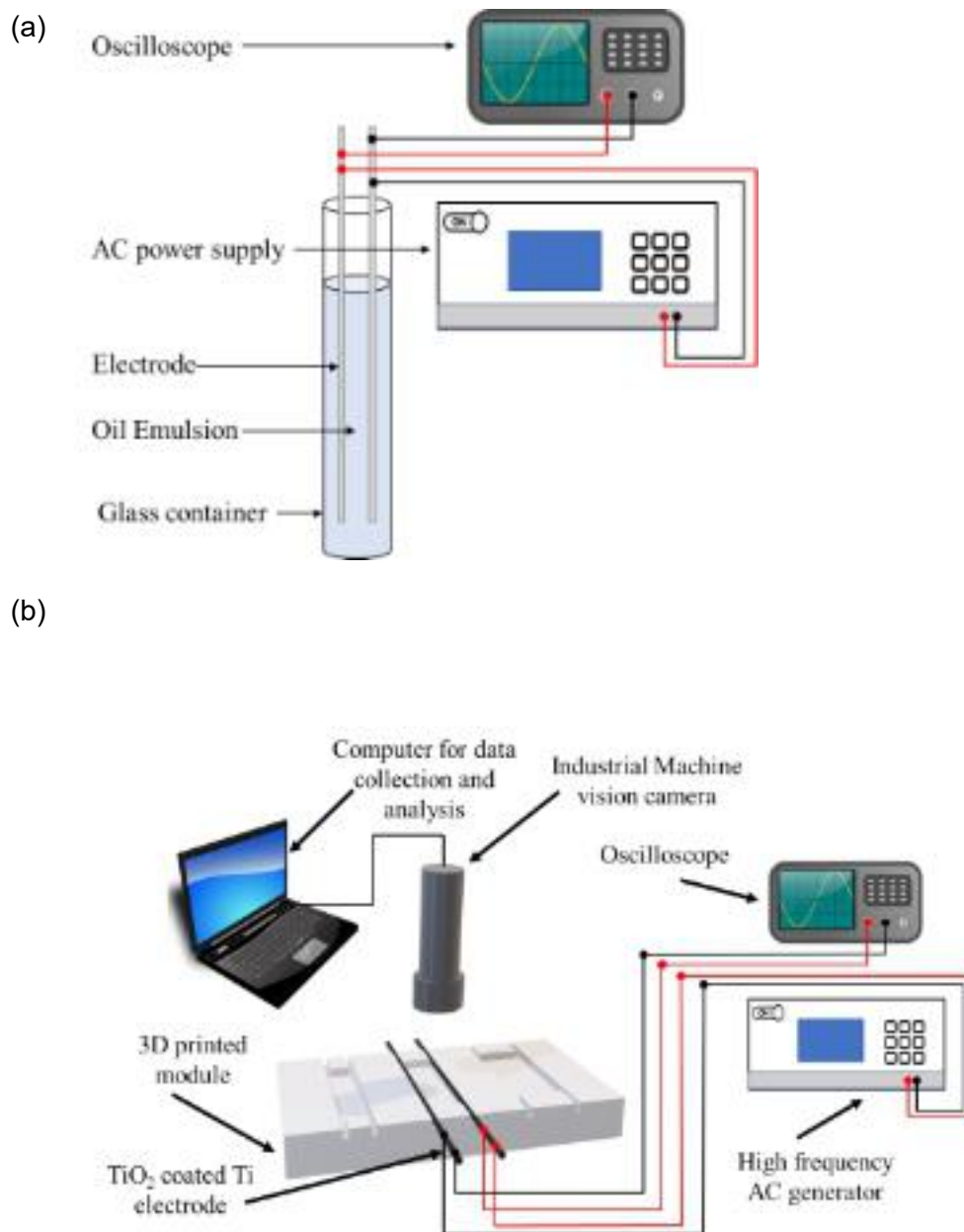
184

185   **Figure 1.** (a) schematics of the experimental setup, (b) droplet coalescence observation setup.

186 3. Numerical Analysis

187 Dielectrophoresis (DEP) is an electrokinetic effect of translational motion of neutral or charged

188 particles instigated by dielectric polarization in an inhomogeneous electric field [22]. The

189 dielectrophoretic force (F_{DEP}) due to the non-uniform electric field on the produced dipole moment

190 of the particle is dependent on the dielectric properties and size of the particle, the frequency of

191 the applied field, and the electrical properties of the medium [23]. The DEP force acting on a

192 spherical particle can be calculated as [24]:

$$F_{DEP} = 4\pi a^3 \varepsilon_0 \varepsilon_M re\left[\widetilde{K}\right](E \cdot \nabla)E \tag{2}$$

193 Here, a is the radius of the particle (m), ε_0 is the permittivity of free space ($8.854 \times 10^{-12} \frac{F}{m}$), ε_M is

194 the relative permittivity of the medium (F/m) , E is the field intensity ($\frac{V}{m}$) and $re\left[\widetilde{K}\right]$ is the real part

195 of Clausius-Mossotti (CM) factor, which is calculated as [23]:

$$\widetilde{K} = \frac{\widetilde{\varepsilon_p} - \widetilde{\varepsilon_M}}{\widetilde{\varepsilon_p} + 2\widetilde{\varepsilon_M}} \tag{3}$$

$$\widetilde{\varepsilon} = \varepsilon - \frac{j\sigma}{\omega} \tag{4}$$

196 Here, $\widetilde{\varepsilon_p}$ is the complex permittivity of the particle (F/m), $\widetilde{\varepsilon_M}$ is the complex permittivity of the

197 medium (F/m), $\widetilde{\varepsilon}$ is the complex permittivity (F/m), σ is the conductivity ($\frac{S}{m}$), $\omega = 2\pi f$ is the angular

198 frequency ($\frac{rad}{s}$), f is the frequency (Hz), $j = \sqrt{-1}$, the geometric gradient of the square of the

199 electric field (E, V/m) is calculated by [23]:

$$(E \cdot \nabla)E = \frac{1}{2}\nabla|E|^2 \tag{5}$$

200 As presented in Equation 2, the gradient of the square of the electric field can be used as an

201 indicator of the DEP force in a DEP system with given properties of particle and medium.

202 Therefore, the gradient of the square of the electric field was simulated to present the impact of

13

203   the different parameters on the demulsification efficiency. Numerical analysis using COMSOL

204   Multiphysics 5.5 was performed to predict the electric field strength generated at different inputs

205   of voltage (*U, volt*) and different inter-electrode distances (*d, meter*).

206   The sketch for the simulated geometry is shown in Figure 2 (a). The simulation was conducted in

207   two dimensions, assuming that the height of the electrode is infinite. The electric potential was

208   solved at a set of boundary conditions to calculate the gradient of the square of the electric field.

209   The medium between the electrodes was assumed to be oil with a known specific conductivity.

210   This assumption was made because the medium is a continuous phase of oil with minute water

211   droplets behaving as particles. To solve this problem for the applied currents and frequencies,

212   the quasi-electrostatic form was used. The root mean square (rms) of the electric field is given

213   by:

$$E = -\nabla\varphi \tag{6}$$

214   Here, φ is the rms of the electrostatic potential which can be given by Laplace's equation

215   (assuming that the medium is liquid only with the absence of any particles and it is homogeneous):

$$\nabla^2\varphi = 0 \tag{7}$$

216   Fixed boundary conditions were applied on the surface of the charge carrying electrodes:

$$\varphi_1 = U_o \tag{8}$$

$$\varphi_2 = 0 \tag{9}$$

217   Here, U_0 is the rms of the oscillating potential drop (volt). An 'extremely fine' mesh was applied to

218   carry out the simulations. To further improve the accuracy of the results, the mesh size can be

219   reduced.

14
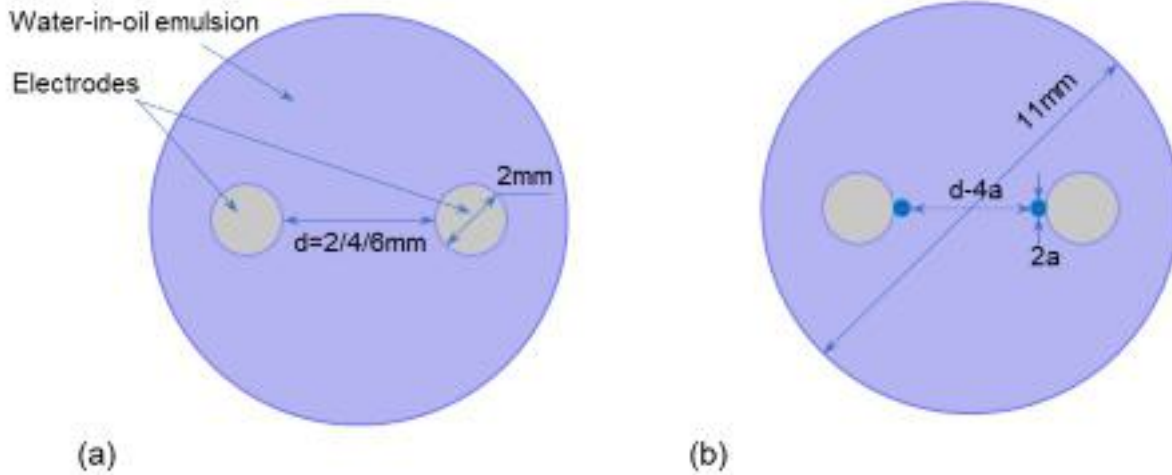
Figure 2. (a) Sketches of the geometry considered in the simulation of the two electrodes (b) the considered geometry for the simulation of the entrapment of water droplets (blue circles) on the surface of the electrodes (gray circles).

To study the influence of trapped water droplets on the surface of the electrodes on the electric field strength, two water droplets of radius 'a' were placed on the surface of each electrode, between the two electrodes (Figure 2 (b)). Although the TiO_2 film is resistive with a conductivity of $10^{-13}\Omega^{-1}cm^{-1}$, high frequency signal can pass though the film. During this study, the range of frequency was between 175 and 250 kHz. At this high frequency, the electric field in the system is not affected by the isolation film. This can result in formation of charges on the surface of the trapped droplets. The numerical analysis on the geometric model was performed using the similar assumptions (i.e. continuous oil medium and infinite electrode height) and similar boundary conditions given in Eqs. (8) and (9). Due to the significantly higher conductivity of water droplets compared to that of oil (continuous phase), electrodes and water droplets together are considered to be one conducting body and forms a new electrodes pair as soon as the water droplets are trapped on the surface of electrodes. The trapped water droplets are therefore assumed to be a protruding point out of electrode surface. The gravity force will move the formed water droplets

238   downward when the radius of the water droplets exceeds 0.1 mm [25]. Hence, this is the largest

239   radius of water droplets that would be trapped on the electrodes and is considered in our

240   simulation.

241   3.2 Results of numerical analysis

242   The numerical analysis to study the effect of voltage on the DEP force was carried out at an inter-

243   electrode distance of 4 mm with four different voltages of 100, 150, 200 and 250 V. The DEP

244   force represented as the gradient of the square of the electric field is shown in Figure 3. As shown

245   in Figure 3, the area under the influence of DEP force increases with increasing voltage. The

246   maximum gradients of the squared electric field were 2×10^{12}, 4.5×10^{12}, 8×10^{12} and $1.3 \times$

247   10^{13} V^2/m^3, for the applied voltages of 100, 150, 200 and 250 V, respectively. Moreover, for all

248   the applied voltages, the gradient of the squared electric field intensity decays very rapidly away

249   from the electrode surface, reaching approximately 0 V^2/m^3 at a distance of 1.4 mm away from

250   the electrode surface. This implies that the maximum DEP force is located in the vicinity of the

251   surface of the electrodes, while the minimum and even null DEP force is located at the midpoint

252   between the two electrodes.

(a)   (b)

(c)

(d)

(e)
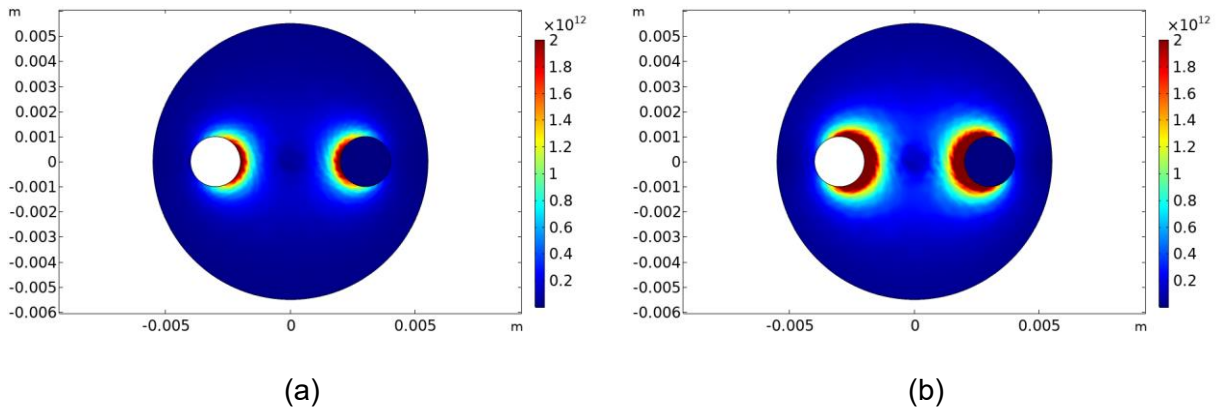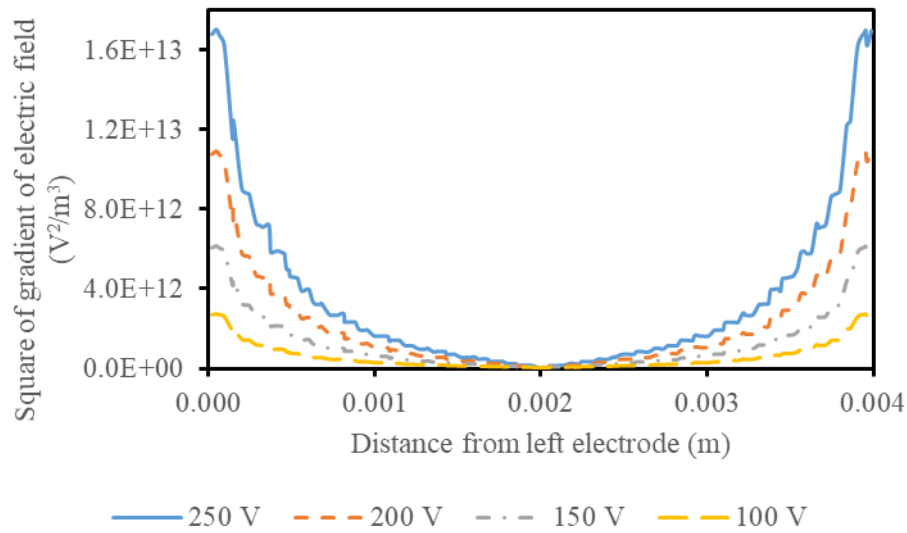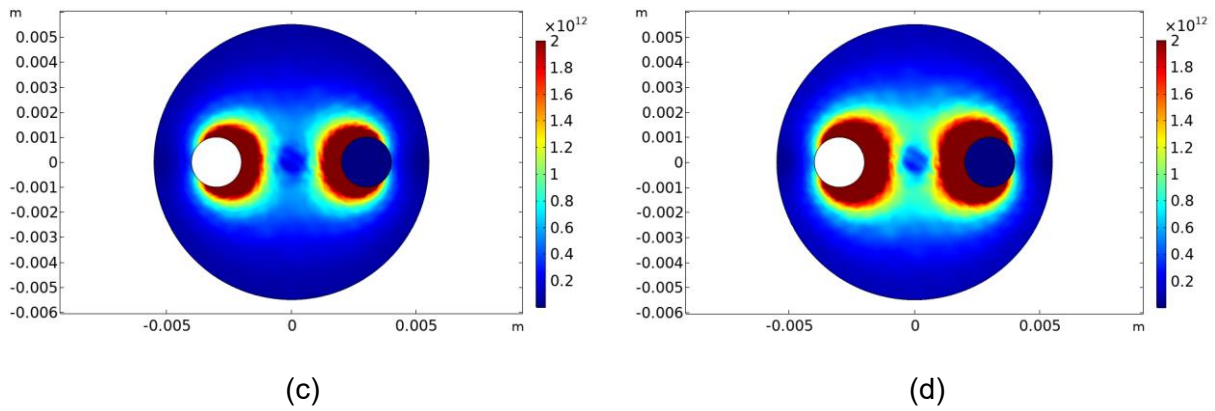
Figure 3. The DEP force field distribution defined as $(\nabla|E|^2)$ for four applied voltages (a) 100 V (b) 150 V (c) 200 V (d) 250 V (e) Squared of the gradient of electric field intensity between the electrodes at different applied voltages (inter-electrode distance 4 mm, frequency 200 kHz).

The numerical analysis to study the effect of the inter-electrode distance on the DEP force was carried out at 250 V with three different inter-electrode distances of 2, 4 and 6 mm. The DEP force represented as the gradient of the square of the electric field is shown in Figure 4. As shown in Figure 4, the area under the influence of DEP force increases with decreasing the distance. The maximum gradients of the squared electric field were 0.9×10^{12}, 1.2×10^{13}, and 3.75×10^{13} V^2/m^3, for inter-electrode distances of 6 mm, 4 mm, and 2 mm, respectively. Moreover, for all the

17

262 inter-electrode distances, the gradient of the squared electric field decays very rapidly away from

263 the electrode surface, reaching approximately 0 V^2/m^3 at a distance of 0.8 mm away from the

264 electrode surface for an inter-electrode distance of 2 mm and at a distance of 1.3 mm away from

265 the electrode surface for inter-electrode distances of 4 mm and 6 mm (Figure 4 (d)).

266

(a)

(b)

(c)

(d)
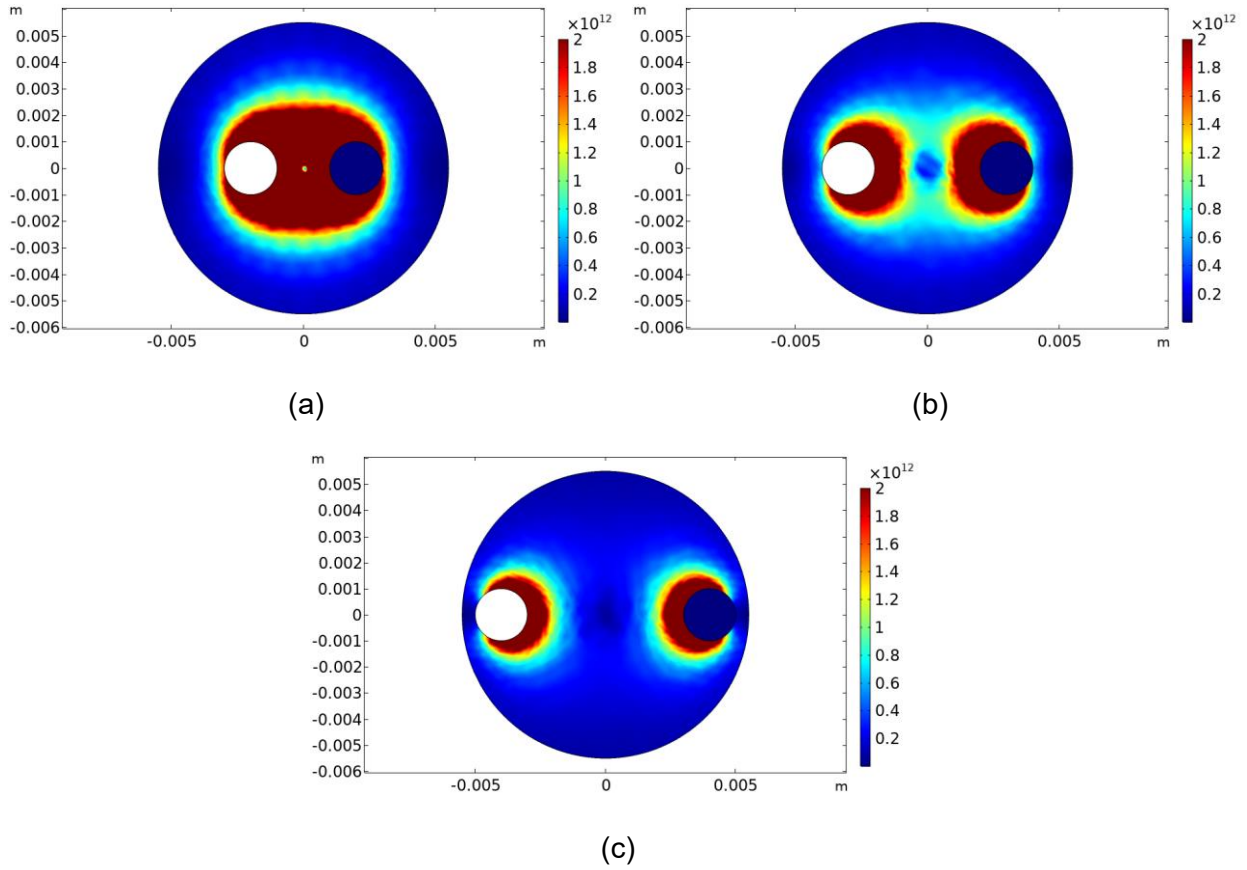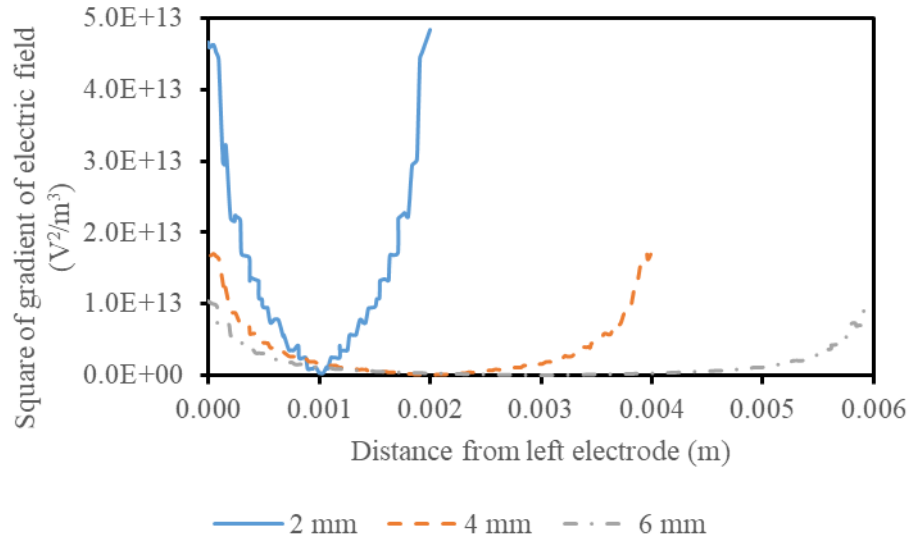
Figure 4. The DEP force field distribution defined as ($\nabla|E|^2$) for inter-electrode distances of (a) 2 mm (b) 4 mm (c) 6 mm (d) Squared of the gradient of electric field intensity between the electrodes at different inter-electrode distance (applied voltage 250 V, frequency 200 kHz).

The influence of the entrapment of water droplets on the surface and between the electrodes on the electric field strength was simulated and compared with the electric field strength generated without water droplets trapped on the electrodes surface (Figure 5). The simulation was performed at two different inter-electrode distances of 2 mm and 4 mm. It can be seen from Figure 5 that for the two inter-electrode distances, 2 mm and 4 mm, the electric field strengths with no water droplets attached to the surface of the electrodes are less than those with water droplets attached to the surface of the electrodes. The impact of the attached water droplets to the surface of the electrodes on enhancing the electric field can be obviously seen as the protruded electric field distribution shown in Figure 5 (c), and quantitatively demonstrated in Figure 5 (b) and (d). The electric field strengths in both electrode arrays with water droplets trapped on the surface of the electrodes are largely enhanced. The maximum electric field strengths were increased about 110% and 106% for inter-electrode distances of 2 mm and 4 mm, respectively. Compared to the

282 homogenous distribution of charges on the surface of the electrodes with no water droplets

283 trapped, more charges are aggregated at the tips of the water droplets, and hence inducing a

284 very inhomogeneously distributed electric field with the maximum electric field strength located at

285 the tips of the water droplets. Eow et al. suggested that an electric field intensity of 300 kV/m and

286 more would cause water droplets to break up and re-emulsify the system and therefore the reduce

287 the demulsification efficiency, the voltage that results in an electric field intensity of 300 kV/m is

288 therefore defined as threshold voltage [26]. It can be seen from Figure 5 (d) that even with the

289 trapped water droplets, the maximum electric field strength generated by the electrode array with

290 distance *d* of 4 mm is still far lower than the threshold electric field intensity. Therefore, the water

291 droplets although trapped on the electrodes surface are expected not to be broken up before they

292 settle down by gravitational force. However, the electric field strength in the vicinity of the water

293 droplets attached to the electrodes is higher than the threshold in the 2 mm distanced electrode

294 array (Figure 5 (b)). Therefore, we could expect a break-up phenomenon occurring and hence a

295 lower demulsification efficiency at an applied voltage of 250 V.

296

(a)   (b)

(c)　　　　　　　　　　　　　　　(d)
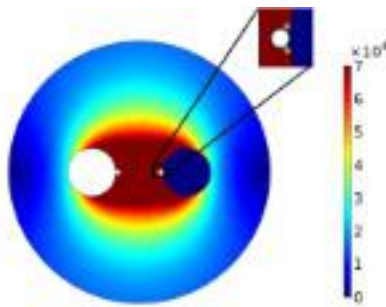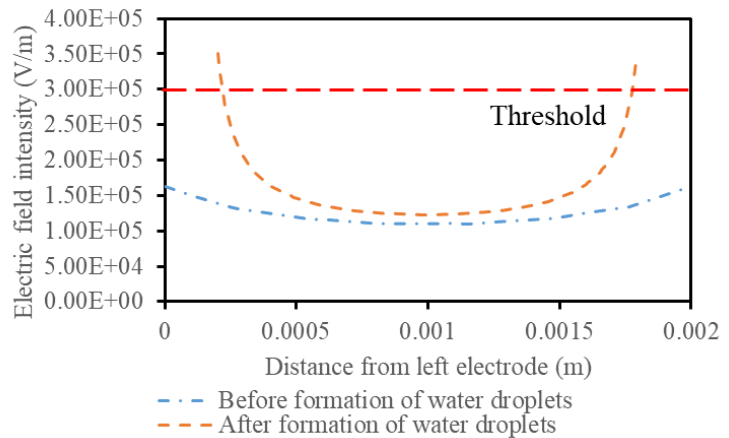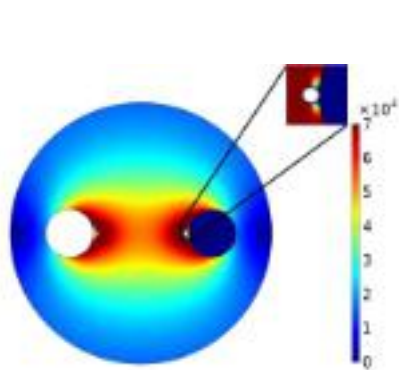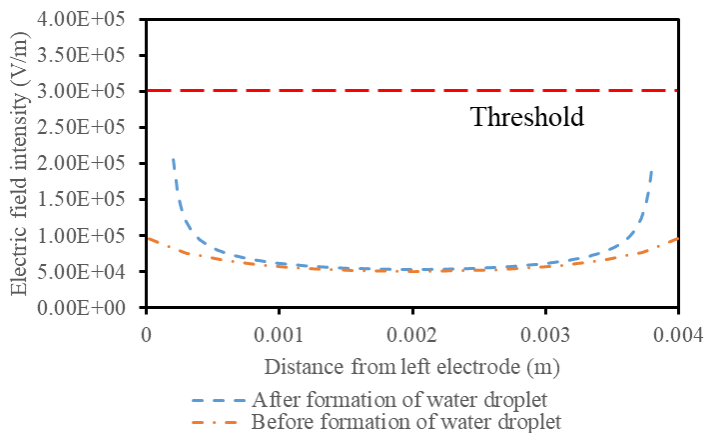
Figure 5. Comparison of electric field between two electrodes (white and blue large circles) with and without water droplet (white small circles) trapped on electrodes surface with an inter-electrode distance of 2 mm (a, b), 4 mm (c, d) (applied voltage 250 V, frequency 200 kHz).

4. Experimental results and discussion

4.1 Effect of electric field strength

The efficiency of electro coalescence is mainly dependent on the electric field strength, which determines the velocity of water droplets and the intensity of their collision. Applied voltage and inter-electrodes distance are two key parameters influencing the electric field strength. The influence of voltage on the demulsification efficiency was experimentally examined with varied voltages of 100, 150, 200 and 250 V, at a constant frequency of 200 kHz and an inter-electrode distance of 4 mm. As shown in Figure 6, higher voltage presents better demulsification efficiency. An applied voltage of 250 V presented the best demulsification efficiency, where after 60 minutes of demulsification time the demulsification efficiency reached 76.1%, while the lowest demulsification process occurred with the lowest applied voltage of 100 V. The improvement of demulsification with increased voltage was also observed by Kim et al. (2002) and Ramadhan et

21

313　al. (2023) [27, 28]. Kim et al. (2002) increased the applied voltage from 1 kV/m to 5 kV/m and

314　improved the demulsification efficiency by 28%, whereas Ramadhan et al. (2023) increased the

315　voltage from 1000 V to 4000 V and improved the demulsification efficiency by 18%. The strength

316　of the DEP force field is directly proportional to the gradient of squared electric field and hence

317　the square of the applied voltage. At higher voltages it is expected that the water droplets in the

318　emulsion will be more affected by the DEP force and thereby experience more coalesce [29]. That

319　also explains why the demulsification efficiency at 250 V increases rapidly compared to the other

320　applied voltages and achieves a relatively stable demulsification efficiency after 45 minutes. The

321　DEP force is expected to promote frequent collision of the water droplets, due to these collisions,

322　the water droplets coalesce forming bigger water droplets, when the radius of the droplets

323　increases to 0.1 mm or more, the droplets will separate from oil under the influence of the

324　gravitational force [25]. Moreover, it was noticed that the application of voltage was accompanied

325　with an increase in temperature of the emulsion where the emulsion temperature increased from

326　22°C to 34°C after 60 min when applying 250 V. This increase of temperature could facilitate the

327　collision of water droplets and increase the efficiency of the demulsification process [30]. In

328　addition, the fact that the maximum demulsification efficiency occurred while applying the highest

329　voltage, implies that no water droplets break-up occurred. The simulation results showed that

330　water droplets will not break-up at an applied voltage of 250 V, a frequency of 200 kHz, and an

331　inter-electrode distance of 4 mm (Figure 5 (d)).
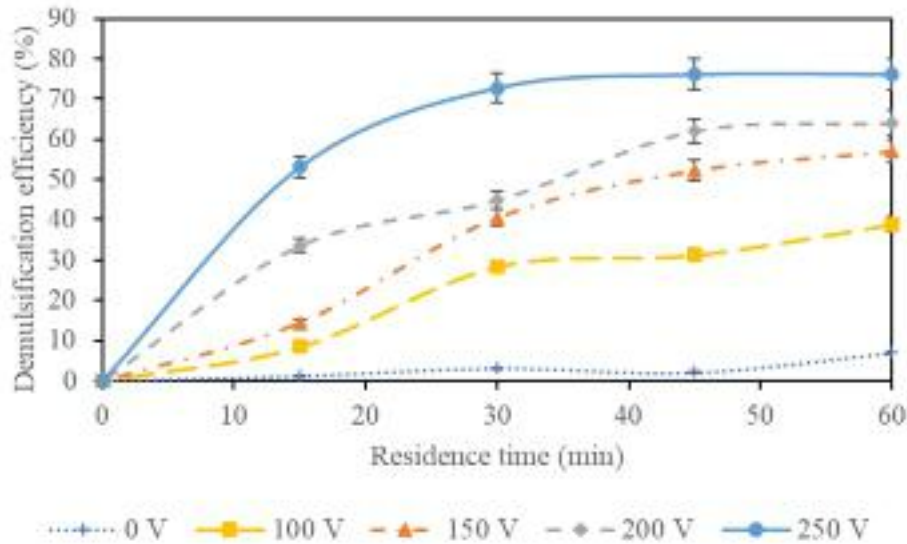
Figure 6. Effect of applied voltage on water removal efficiency (inter-electrode distance 4 mm, frequency 200 kHz).

4.2 Effect of inter-electrode distance

The effect of the inter-electrode distance on the demulsification efficiency was studied by analyzing the demulsification efficiency at three different inter-electrode distances of 2 mm, 4 mm and 6 mm. The applied voltage and frequency were fixed at 250 V and 200 kHz, respectively. As shown in Figure 7, the demulsification efficiency at an inter-electrode distance of 4 mm was the highest. Comparing the 4 mm inter-electrode distance to the 6 mm inter-electrode distance, the induced electric field is stronger for the case of the shorter distance, which could enhance the DEP force and hence the number of collisions of water droplets, thereby presenting higher demulsification efficiency. According to the simulation results shown in Figure 4, the highest electric field strength and hence the highest DEP force are generated at an inter-electrode distance of 2 mm. However, contrary to the simulation results using an inter-electrode distance of 2 mm resulted in a lower demulsification efficiency compared to an inter-electrode distance of 4 mm. It can be seen from Figure 11 that at the 60th minute the demulsification efficiency for the 2 mm inter-electrode distance was 14% lower than the 4 mm inter-electrode distance. The very

23

349 strong DEP force when using the 2 mm inter-electrode distance allows water droplets around the

350 electrodes to be rapidly moved to and trapped on the surface of the electrodes. Trapped water

351 droplets, although still small, could enhance the electric field strength and the DEP force for

352 attracting more water droplets on these already trapped water droplets and thereby growing very

353 fast. As presented in the numerical analysis (Figure 5 (a) and (b)), as soon as the radius of the

354 water droplets grows up to 100 μm, the electric field intensity at the surface of the electrode

355 increases by 109.58% and reaches 350 kV/m, which is much higher than the threshold of 300

356 kV/m [26]. Due to this high electric field intensity, these 100 μm water droplets will be ruptured

357 immediately to release secondary much smaller water droplets [26]. Such re-generated small

358 water droplets will re-emulsify the system and therefore the demulsification efficiency is largely

359 reduced. In the case of the 4 mm inter-electrode distance the induced electric field is far lower

360 than the threshold of 300 kV/m as shown in the simulation results in Figure 5 (c) and (d). The

361 demulsification process and the accumulation of the water droplets on the surface of the electrode

362 can be clearly seen in Figure 8. Figure 8 (a) shows how the water droplets are dispersed in oil

363 before the application of the electric field while Figure 8 (b) shows how the water droplets formed

364 are accumulated on the surface of the electrode after the application of the electric field.

365

366

367

368
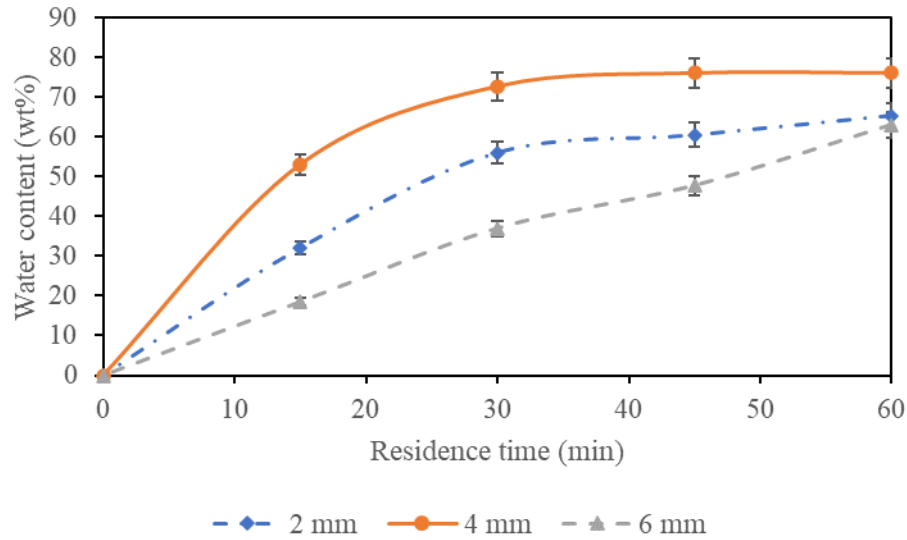
Figure 7. Effect of electrode distance on demulsification efficiency (applied voltage 250 V, frequency 200 kHz).

(a)   (b)
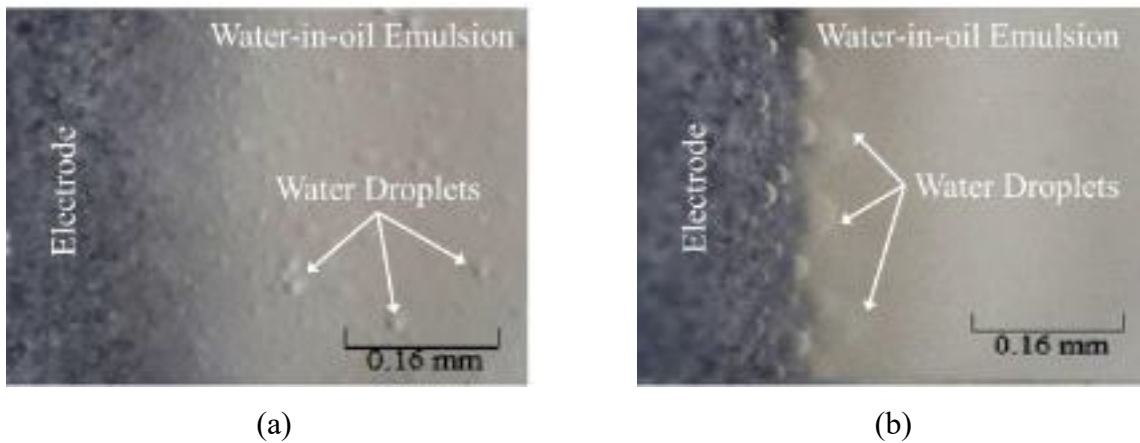
371 **Figure 8.** The water-in-oil emulsion (a) no applied electric field (b) with applied electric field with
372 an applied voltage of 250 V, frequency of 200kHz, and an inter-electrode distance of 4mm after
373 45 minutes demulsification time. (The brightness and contrast of the image has been digitally
374 improved)

375 4.3 Effect of frequency

376 The effect of frequency on the demulsification efficiency was studied by analyzing the
377 demulsification efficiency at four different high frequencies of 175, 200, 225 and 250 kHz and

378   one low frequency of 50 Hz. The applied voltage and inter-electrode distance were fixed at 250 V

379   and 4 mm, respectively. The application of high frequency is on one hand to avoid the

380   electrochemical reaction on the surface of the metal electrodes and on the other hand to prevent

381   the formation of the pearl-chain, which might induce a short circuit of the system and hence largely

382   reduce the demulsification efficiency and even damage the demulsification system. It can be seen

383   from Figure 9 that all examined high frequencies presented very similar tendency where the

384   difference on the demulsification efficiencies is very insignificant. However, at a very low

385   frequency of 50 Hz, the demulsification efficiency was poor at only 9.8% compared to a maximum

386   demulsification efficiency of 72.6% at a frequency of 200 kHz (Figure 10). In the literature, Kim et

387   al. (2002) and Ramadhan et al. (2023) also observed improved demulsification efficiency at

388   elevated frequencies of 1000 Hz and 1500 Hz, respectively [27, 28]. Ramadhan et al (2023)

389   observed a 55% improvement in demulsification efficiency while increasing the frequency from

390   50 Hz to 2000 Hz, whereas Kim et al. (2002) obtained 13% improvement in demulsification

391   efficiency by increasing frequency from 50 Hz to 2000 Hz. Frequency is believed to be one of the

392   most important parameters that would affect the chain formation of water droplets during

393   demulsification [31]. With very high frequency, the charges on the water droplets will not have

394   sufficient time to respond to the electric field and hence the water droplets will migrate for

395   coalescence. In addition, when compared to DC voltage, the demulsification efficiency obtained

396   by applying high frequency AC voltage was 37% higher. This indicates that in DC the

397   demulsification process is dominated by electrophoresis and the dielectrophoretic force is only

398   dominant when higher frequency AC voltage is applied. Moreover, the better demulsification

399   performance of AC voltage at 200 kHz compared to DC is attributed to the induction of more

400   droplet-droplet collision at high frequency AC voltage and prevention of pearl chain formation [26,

401   32].

402
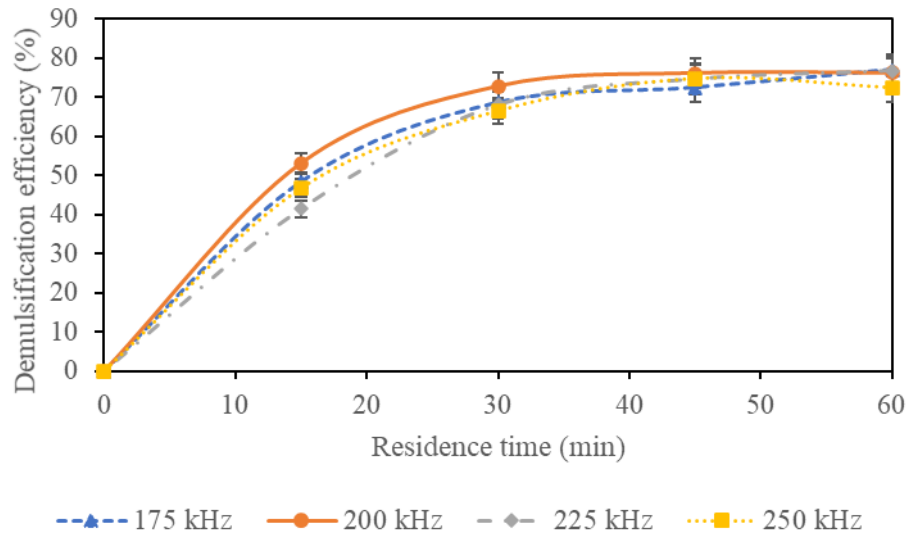
Figure 9. Effect of AC frequency on water removal efficiency (inter-electrode distance 4 mm,

404   voltage 250 V).
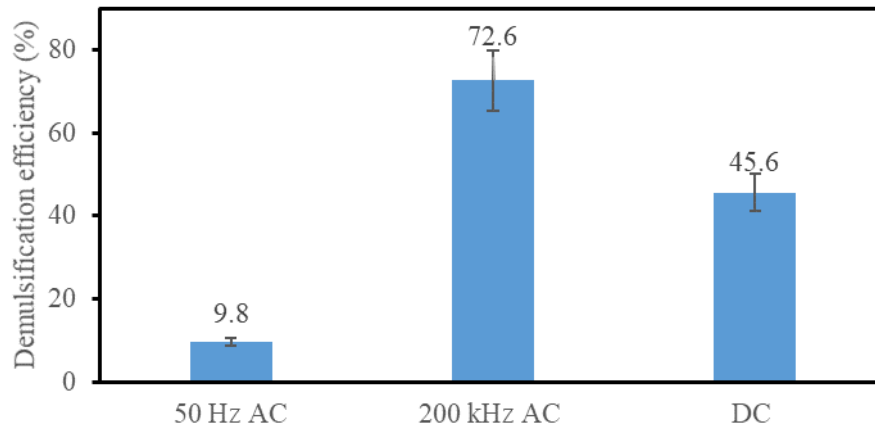
405

406   **Figure 10.** Effect of frequency and different types of power supply on demulsification efficiency.

407   4.4 Energy analysis

408   The specific energy consumption of the demulsification process was calculated as:

$$E = \frac{U \times I \times t}{1000 \times V} \tag{15}$$

409   Here, E is the specific energy requirement of the process (kWh/L), U is voltage (V), I is current

410   (A), t is time (h) and V is the volume (L) of the water-in-oil emulsion. 1000 is the conversion factor

411   used to convert watt-hr to kilowatt-hr. The voltage (U) and current (I) were continuously measured

412   using an oscilloscope. The specific energy consumption was calculated for an inter-electrode

413   distance of 4 mm and a frequency of 200 kHz. In order to compare the energy consumption at

414   different applied voltages, the maximum demulsification efficiency of the lowest applied voltage

415   was used as the base line. As shown in Figure 6 a maximum demulsification efficiency of 39%

416   was achieved after 60 minutes with an applied voltage of 100 V. The same demulsification

417   efficiency was achieved after 30, 15 and 8 minutes with an applied voltage of 150, 200 and 250

418   V, respectively. Figure 11 shows that the specific energy consumption for a demulsification

419   efficiency of 39% was 0.223, 0.176, 0.174, and 0.124 kWh/L at an applied voltage of 100, 150,

420   200, and 250 V, respectively. The lowest specific energy consumption was achieved with the

421   highest applied voltage due to the much lower time required to reach the targeted demulsification

422   efficiency. Table 3 shows the specific energy consumption of different demulsification strategies

423   that are being developed. As seen in Table 3, the specific energy consumption obtained from this

424   study is 4.0, 54.8 and 16.9 times lower than the specific energy consumption of centrifugation,

425   microwave irradiation and electrocoagulation based demulsification processes, respectively [33-

426   35].

427

428
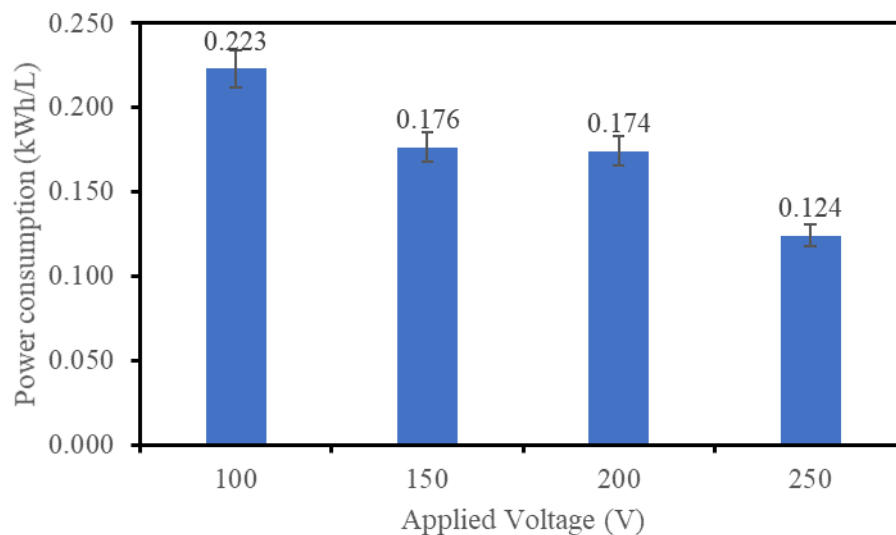
429

430   **Figure 11.** Specific power consumption at different applied voltages (39% demulsification

431   efficiency, inter-electrode distance 4 mm, frequency 200 kHz).

432   **Table 3.** Comparison of energy consumption of different technologies.

Demulsification Technology	Specific energy consumption (kWh/L)	Reference
Miniaturized centrifugal demulsification device	0. 49	[35]
Microwave irradiation assisted demulsification	6.80	[34]
Parallel-plate electrocoagulation	2.1	[33]
Electro-coalescence using TiO_2 coated electrodes	0.124	This study

433

4.5 Comparison with previous studies

Table 4 shows comparison of electro-coalescence performance between this study and other studies. As seen from Table 4, the 76% demulsification efficiency obtained from this study is one of the highest. Higher demulsification efficiency of 82.5% was obtained by Hu et al. (2021) for an emulsion containing 90 v% water [36]. The higher water content means higher number of water droplets to collide and coalesce which resulted in higher demulsification efficiency in the study. For a water content of 20%, Kim et al. (2002) designed and used a hydrostatic demulsifier to obtain 90% demulsification efficiency while using 200 ppm Betzdearborn as chemical demulsifier [27]. The improved demulsification efficiency in the study is attributed to the chemical demulsifier since the same study reported 0% demulsification without addition of demulsifier. Compared to other studies that has achieved greater than 70% demulsification efficiency, the current study used lower applied voltage and demulsification time. Ramadhan et al. (2023) obtained 75% demulsification efficiency within 60 mins of demulsification time, however, the reported applied voltage was 4000 V [28]. On the other hand, Taleghani et al. (2019) needed 50 hours to achieve 58% demulsification efficiency [37].

450 **Table 4.** Comparison of electrocoalescence performance with previous studies.

Emulsion	Applied voltage	Frequency	Demulsification Time	Demulsifier	Demulsification efficiency	Reference
20 v% water 80 v% crude oil	2.5 kV/cm	60 Hz	3 min	75 ppm Betzdearborn	60%	[27]
		60 Hz	3 min	N/A	0%	
32.2% water 13.9 v% light oil 30.3 v% heavy oil 23.6 v% solids	2.05 V/cm	N/A	50 hrs	N/A	44%	[37]
		N/A	50 hrs	3452 ppm FeCl$_3$	58%	
		N/A	50 hrs	3452 ppm alum	17%	
10 v% water 90 v% castor oil	4000 V	1500 Hz	60 mins	N/A	20%	[28]
10 v% water 90 v% soyabean oil	4000 V	1500 Hz	60 mins	N/A	75%	
90 v% water 10 v% kerosene	150 V	1000 Hz	11 min	N/A	82.5%	[36]
4.71 wt% water 95.29 wt% lubricant	250 V	200 kHz	45 min	N/A	76%	This work

5. Conclusion

In this work we numerically simulated and experimentally demonstrated the influence of electric field on the demulsification efficiency by varying the electric field determining parameters (including voltage, frequency and distance between electrodes). It was found that trapped water droplets on the electrodes surface could largely influence the electric field strength, and hence the demulsification process. The entrapped water droplets become a part of the electrode and thereby forming a new electrodes pair. The new electrodes pair has a shorter inter-electrode distance and therefore stronger electric field strength is generated with unchanged applied voltage. With the growth of the water droplets due to the electrocoalescence, the inter-electrode distance is further reduced and the induced electric field increases. When the induced electric field strength is below the threshold of 300 kV/m, the demulsification efficiency could be enhanced by increasing the electric field either through applying higher voltage or reducing the distance between electrodes. However, if the induced electric field is above 300 kV/m, the trapped water droplets will be broken up, and hence releasing many much smaller water droplets, which re-emulsifies the system and hence largely reduces the demulsification efficiency. We numerically simulated and experimentally validated such an effect using a 2 mm distanced electrodes array with the application of voltage of 250 V and frequency of 200 kHz. Due to the trapped water droplets on electrodes, the electric field was largely increased about 109.58% to 350 kV/m far beyond the threshold and hence resulted in the lower demulsification efficiency of 65%.

With this new understanding, a maximum demulsification efficiency of 76% was obtained by optimally applying the parameters of 250 V for voltage, 200 kHz for frequency, 4 mm for the inter-electrode distance, in a 45 min process with the most efficient energy consumption of 0.51 kWh/L. The application of high frequency and the utilization of insulation are suggested for avoiding of

475 the electrochemical reaction on the electrodes and preventing from the generation of gas bubbles

476 as well as the pearl-chain formation of water droplets.

477 We found that the demulsification efficiency using high frequency AC electric field was 37% higher

478 than when using DC field with other parameters constant. This is due to the much stronger

479 collision and hence coalescence between water droplets driven by the DEP force in AC electric

480 field with high frequency compared to that induced by EP force in DC electric field.

Acknowledgment

References

486 [1] S. F. Wong, J. S. Lim, and S. S. Dol, "Crude oil emulsion: A review on formation,
487 classification and stability of water-in-oil emulsions," *Journal of Petroleum Science and*
488 *Engineering,* vol. 135, pp. 498-504, 2015/11/01/ 2015, doi:
489 https://doi.org/10.1016/j.petrol.2015.10.006.
490 [2] Y. Xu *et al.*, "Breaking Water-in-Bitumen Emulsions using Polyoxyalkylated DETA
491 Demulsifier," *The Canadian Journal of Chemical Engineering,* vol. 82, no. 4, pp. 829-835,
492 2004/08/01 2004, doi: 10.1002/cjce.5450820423.
493 [3] O. C. Mullins, "The Asphaltenes," *Annual Review of Analytical Chemistry,* vol. 4, no. 1,
494 pp. 393-418, 2011/07/19 2011, doi: 10.1146/annurev-anchem-061010-113849.
495 [4] G. P. Canevari, "The formulation of an effective demulsifier for oil spill emulsions,"
496 *Marine Pollution Bulletin,* vol. 13, no. 2, pp. 49-54, 1982/02/01/ 1982, doi:
497 https://doi.org/10.1016/0025-326X(82)90441-6.
498 [5] M. Fingas, "Water-in-oil emulsion formation: A review of physics and mathematical
499 modelling," *Spill Science & Technology Bulletin,* vol. 2, no. 1, pp. 55-59, 1995/03/01/
500 1995, doi: https://doi.org/10.1016/1353-2561(95)94483-Z.
501 [6] "Chapter 23 - Demulsifiers," in *Petroleum Engineer's Guide to Oil Field Chemicals and*
502 *Fluids (Second Edition)*, J. Fink Ed. Boston: Gulf Professional Publishing, 2015, pp. 787-
503 808.
504 [7] Y. N. Romanova, T. A. Maryutina, N. S. Musina, and B. Y. Spivakov, "Application of
505 ultrasonic treatment for demulsification of stable water-in-oil emulsions," *Journal of*
506 *Petroleum Science and Engineering,* vol. 209, p. 109977, 2022/02/01/ 2022, doi:
507 https://doi.org/10.1016/j.petrol.2021.109977.

508 [8] M. Cao, F. Xiao, Z. Yang, Y. Chen, and L. Lin, "Construction of Polytetrafluoroethylene
509   nanofiber membrane via continuous electrospinning/electrospraying strategy for oil-water
510   separation and demulsification," *Separation and Purification Technology,* vol. 287, p.
511   120575, 2022/04/15/ 2022, doi: https://doi.org/10.1016/j.seppur.2022.120575.
512 [9] X. Zhu *et al.*, "Multifunctional recycled wet wipe with negatively charged coating for
513   durable separation of oil/water emulsion via interface charge demulsification," *Separation*
514   *and Purification Technology,* vol. 280, p. 119984, 2022/01/01/ 2022, doi:
515   https://doi.org/10.1016/j.seppur.2021.119984.
516 [10] R. Zolfaghari, A. Fakhru'l-Razi, L. C. Abdullah, S. S. E. H. Elnashaie, and A. Pendashteh,
517   "Demulsification techniques of water-in-oil and oil-in-water emulsions in petroleum
518   industry," *Separation and Purification Technology,* vol. 170, pp. 377-407, 2016/10/01/
519   2016, doi: https://doi.org/10.1016/j.seppur.2016.06.026.
520 [11] K. Alinezhad, M. Hosseini, K. Movagarnejad, and M. Salehi, "Experimental and modeling
521   approach to study separation of water in crude oil emulsion under non-uniform electrical
522   field," *Korean Journal of Chemical Engineering,* vol. 27, no. 1, pp. 198-205, 2010/01/01
523   2010, doi: 10.1007/s11814-009-0324-2.
524 [12] J. S. Eow, M. Ghadiri, A. O. Sharif, and T. J. Williams, "Electrostatic enhancement of
525   coalescence of water droplets in oil: a review of the current understanding," *Chemical*
526   *Engineering Journal,* vol. 84, no. 3, pp. 173-192, 2001/12/15/ 2001, doi:
527   https://doi.org/10.1016/S1385-8947(00)00386-7.
528 [13] Y. Zhou, Z. Wang, and Z. Sun, "Formation of water chain under the non-uniform AC
529   electric field," *Chemical Engineering Research and Design,* vol. 177, pp. 65-69,
530   2022/01/01/ 2022, doi: https://doi.org/10.1016/j.cherd.2021.08.025.
531 [14] S. H. Mousavi, M. Ghadiri, and M. Buckley, "Electro-coalescence of water drops in oils
532   under pulsatile electric fields," *Chemical Engineering Science,* vol. 120, pp. 130-142,
533   2014/12/16/ 2014, doi: https://doi.org/10.1016/j.ces.2014.08.055.
534 [15] S. Less, A. Hannisdal, E. Bjørklund, and J. Sjöblom, "Electrostatic destabilization of water-
535   in-crude oil emulsions: Application to a real case and evaluation of the Aibel VIEC
536   technology," *Fuel,* vol. 87, no. 12, pp. 2572-2581, 2008/09/01/ 2008, doi:
537   https://doi.org/10.1016/j.fuel.2008.03.004.
538 [16] B. Li *et al.*, "Electrocoalescence of water droplet trains in sunflower oil under the coupling
539   of Non-uniform electric and Laminar flow fields," *Chemical Engineering Science,* vol.
540   248, p. 117158, 2022/02/02/ 2022, doi: https://doi.org/10.1016/j.ces.2021.117158.
541 [17] M. Hussein and I. Kareem, "Optimising the chemical demulsification of water-in-crude oil
542   emulsion using the Taguchi method," *IOP Conference Series: Materials Science and*
543   *Engineering,* vol. 987, no. 1, p. 012016, 2020/11/01 2020, doi: 10.1088/1757-
544   899x/987/1/012016.
545 [18] F. Ye *et al.*, "Demulsification of water-in-crude oil emulsion driven by a carbonaceous
546   demulsifier from natural rice husks," *Chemosphere,* vol. 288, p. 132656, 2022/02/01/ 2022,
547   doi: https://doi.org/10.1016/j.chemosphere.2021.132656.
548 [19] V. Rajaković and D. Skala, "Separation of water-in-oil emulsions by freeze/thaw method
549   and microwave radiation," *Separation and Purification Technology,* vol. 49, no. 2, pp. 192-
550   196, 2006/04/15/ 2006, doi: https://doi.org/10.1016/j.seppur.2005.09.012.
551 [20] S. Mhatre *et al.*, "Electrostatic phase separation: A review," *Chemical Engineering*
552   *Research and Design,* vol. 96, pp. 177-195, 2015/04/01/ 2015, doi:
553   https://doi.org/10.1016/j.cherd.2015.02.012.

[21] C. M. G. Atehortúa, N. Pérez, M. A. B. Andrade, L. O. V. Pereira, and J. C. Adamowski, "Water-in-oil emulsions separation using an ultrasonic standing wave coalescence chamber," *Ultrasonics Sonochemistry,* vol. 57, pp. 57-61, 2019/10/01/ 2019, doi: https://doi.org/10.1016/j.ultsonch.2019.04.043.

[22] A. H. Hawari *et al.*, "Impact of aeration rate and dielectrophoretic force on fouling suppression in submerged membrane bioreactors," *Chemical Engineering and Processing - Process Intensification,* vol. 142, p. 107565, 2019/08/01/ 2019, doi: https://doi.org/10.1016/j.cep.2019.107565.

[23] F. Du *et al.*, "Fouling suppression in submerged membrane bioreactors by obstacle dielectrophoresis," *Journal of Membrane Science,* vol. 549, pp. 466-473, 2018/03/01/ 2018, doi: https://doi.org/10.1016/j.memsci.2017.12.049.

[24] A. H. Hawari, A. M. Alkhatib, P. Das, M. Thaher, and A. Benamor, "Effect of the induced dielectrophoretic force on harvesting of marine microalgae (Tetraselmis sp.) in electrocoagulation," *Journal of Environmental Management,* vol. 260, p. 110106, 2020/04/15/ 2020, doi: https://doi.org/10.1016/j.jenvman.2020.110106.

[25] J. S. Eow, M. Ghadiri, and A. O. Sharif, "Electro-hydrodynamic separation of aqueous drops from flowing viscous oil," *Journal of Petroleum Science and Engineering,* vol. 55, no. 1, pp. 146-155, 2007/01/01/ 2007, doi: https://doi.org/10.1016/j.petrol.2006.04.005.

[26] J. Eow, M. Ghadiri, and A. Sharif, "Deformation and break-up of aqueous drops in dielectric liquids in high electric fields," *Journal of Electrostatics,* vol. 51, pp. 463-469, 05/01 2001, doi: 10.1016/S0304-3886(01)00035-3.

[27] B.-Y. Kim, J. H. Moon, T.-H. Sung, S.-M. Yang, and J.-D. Kim, "Demulsification of water-in-crude oil emulsions by a continuous electrostatic dehydrator," *Separation Science and Technology,* vol. 37, no. 6, pp. 1307-1320, 2002/04/24 2002, doi: 10.1081/SS-120002613.

[28] M. G. Ramadhan, N. Khalid, K. Uemura, M. A. Neves, S. Ichikawa, and M. Nakajima, "Efficient water removal from water-in-oil emulsions by high electric field demulsification," *Separation Science and Technology,* vol. 58, no. 1, pp. 164-174, 2023/01/02 2023, doi: 10.1080/01496395.2022.2086882.

[29] B. Li, Z. Sun, Z. Wang, Y. Jin, and Y. Fan, "Effects of high-frequency and high-voltage pulsed electric field parameters on water chain formation," *Journal of Electrostatics,* vol. 80, pp. 22-29, 2016/04/01/ 2016, doi: https://doi.org/10.1016/j.elstat.2016.01.003.

[30] B. P. Binks and A. Rocher, "Effects of temperature on water-in-oil emulsions stabilised solely by wax microparticles," *Journal of Colloid and Interface Science,* vol. 335, no. 1, pp. 94-104, 2009/07/01/ 2009, doi: https://doi.org/10.1016/j.jcis.2009.03.089.

[31] J. S. Eow and M. Ghadiri, "Drop–drop coalescence in an electric field: the effects of applied electric field and electrode geometry," *Colloids and Surfaces A: Physicochemical and Engineering Aspects,* vol. 219, no. 1, pp. 253-279, 2003/06/19/ 2003, doi: https://doi.org/10.1016/S0927-7757(03)00051-7.

[32] Y. Higashiyama, T. Yamada, and T. Sugimoto, "Vibration of water droplet located on a hydrophobic sheet under the tangential AC field," in *Conference Record of the 1999 IEEE Industry Applications Conference. Thirty-Forth IAS Annual Meeting (Cat. No.99CH36370)*, 3-7 Oct. 1999 1999, vol. 3, pp. 1825-1830 vol.3, doi: 10.1109/IAS.1999.805987.

[33] Y. Liu, W.-m. Jiang, J. Yang, Y.-x. Li, M.-c. Chen, and J.-n. Li, "Experimental study on evaluation and optimization of tilt angle of parallel-plate electrodes using

599   electrocoagulation device for oily water demulsification," *Chemosphere,* vol. 181, pp. 142-
600   149, 2017/08/01/ 2017, doi: https://doi.org/10.1016/j.chemosphere.2017.03.141.
601   [34]   X. Lv *et al.*, "Study on the demulsification of refinery oily sludge enhanced by microwave
602   irradiation," *Fuel,* vol. 279, p. 118417, 2020/11/01/ 2020, doi:
603   https://doi.org/10.1016/j.fuel.2020.118417.
604   [35]   Y. Wang, C. Du, Z. Yan, W. Duan, J. Deng, and G. Luo, "Rapid demulsification and phase
605   separation in a miniaturized centrifugal demulsification device," *Chemical Engineering*
606   *Journal,* vol. 446, p. 137276, 2022/10/15/ 2022, doi:
607   https://doi.org/10.1016/j.cej.2022.137276.
608   [36]   J. Hu *et al.*, "Dynamic demulsification of oil-in-water emulsions with electrocoalescence:
609   Diameter distribution of oil droplets," *Separation and Purification Technology,* vol. 254,
610   p. 117631, 2021/01/01/ 2021, doi: https://doi.org/10.1016/j.seppur.2020.117631.
611   [37]   S. Taslimi Taleghani, A. Fellah Jahromi, and M. Elektorowicz, "Electro-demulsification
612   of water-in-oil suspensions enhanced with implementing various additives," *Chemosphere,*
613   vol. 233, pp. 157-163, 2019/10/01/ 2019, doi:
614   https://doi.org/10.1016/j.chemosphere.2019.05.161.

615

616

Supplementary Data
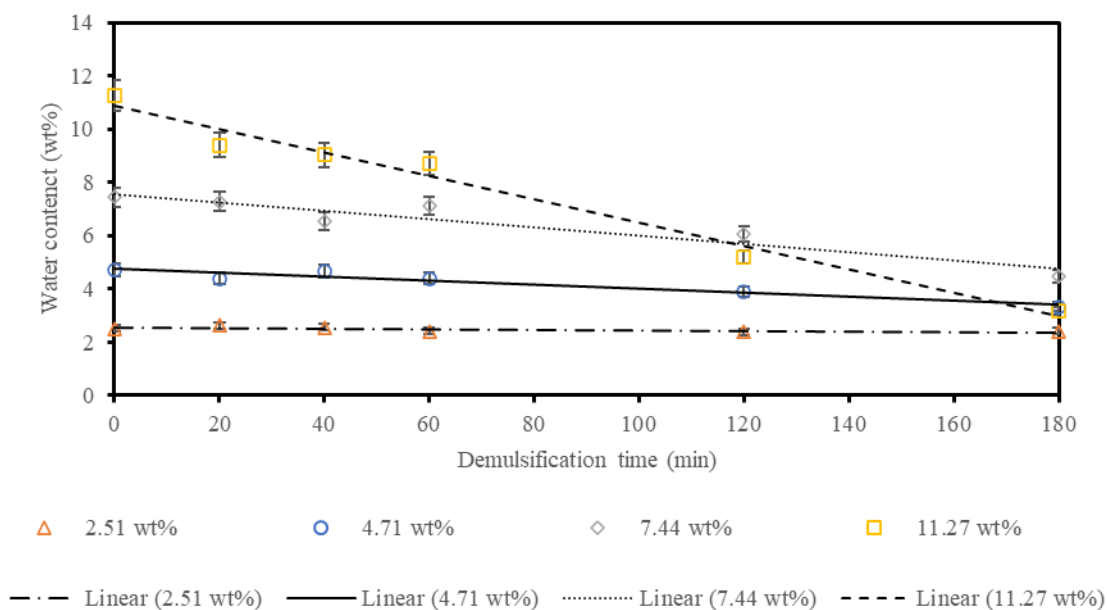
Figure S1. Effect of water content on water-in-oil emulsion stability (10,000 RPM, 5 min).
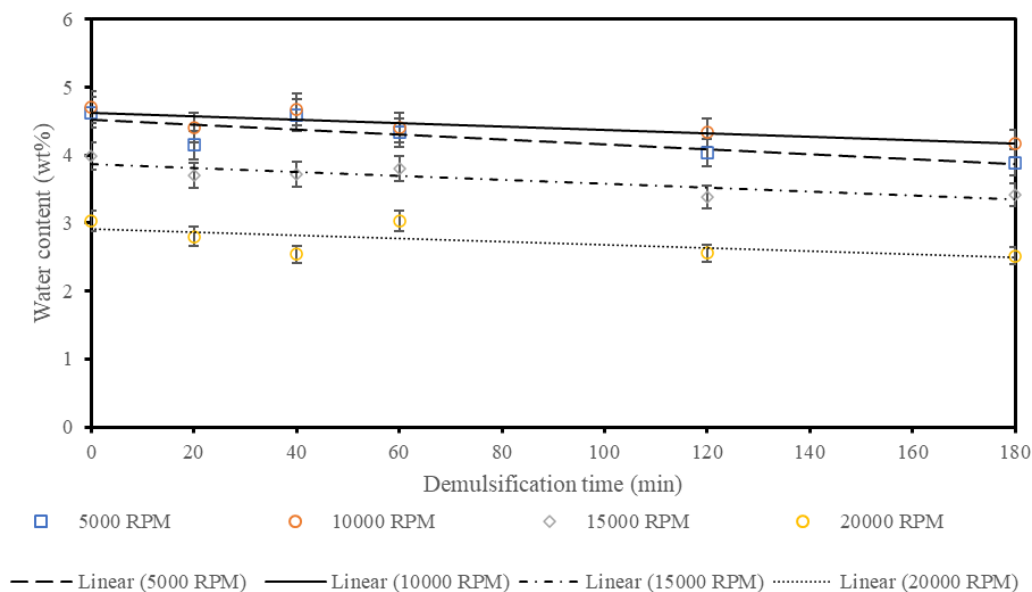
Figure S2. Effect of dispersion speed on water-in-oil emulsion stability (5 mins, 4.71 wt%).
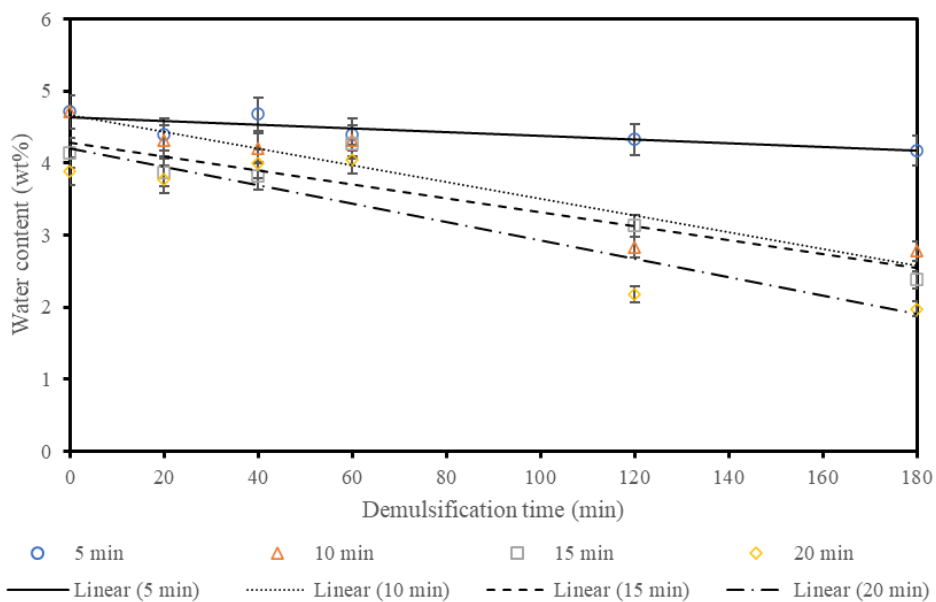
622

623 **Figure S3.** Effect of dispersion time on water-in-oil emulsion stability (10,000 RPM, 4.71 wt%).
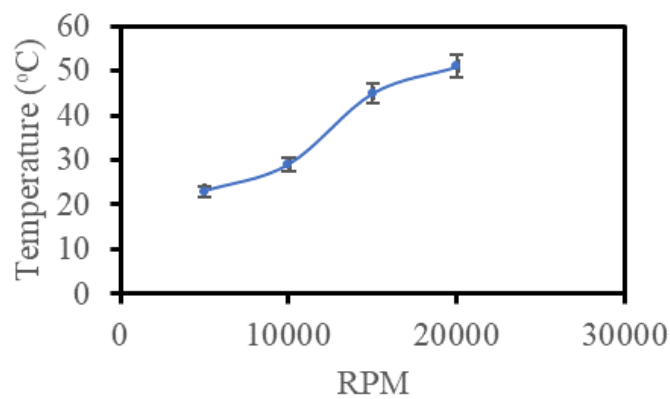
624 **Figure S4.** The temperature of the emulsion after 5 min of emulsification at different dispersion
625 speeds.

Average droplet size: 291 nm
(a)

Average droplet size: 358 nm
(b)

Average droplet size: 481 nm
(c)
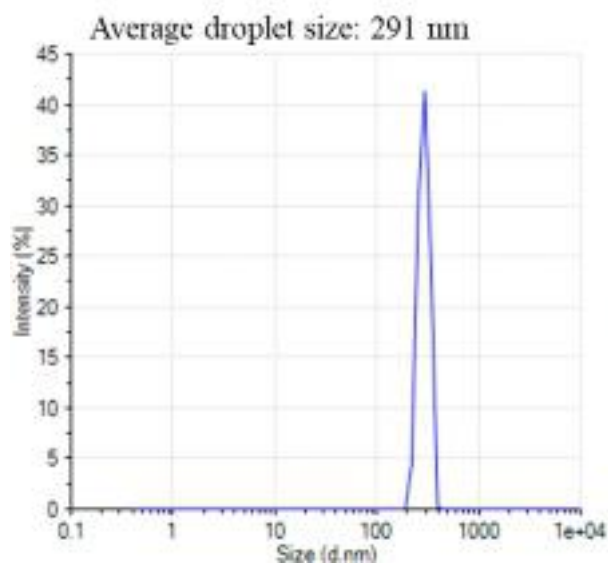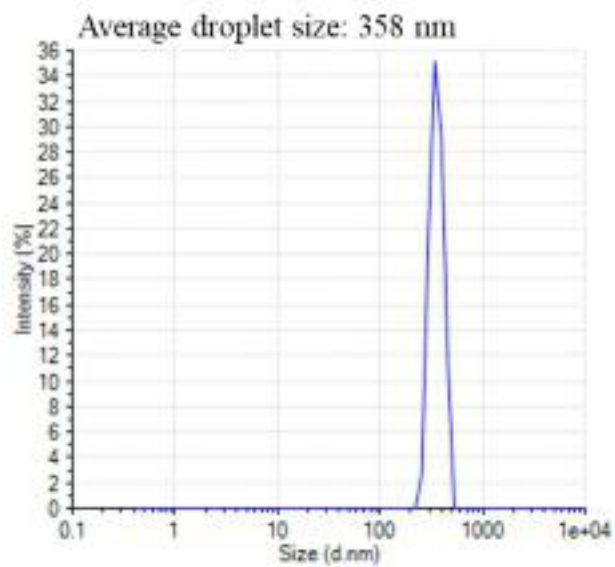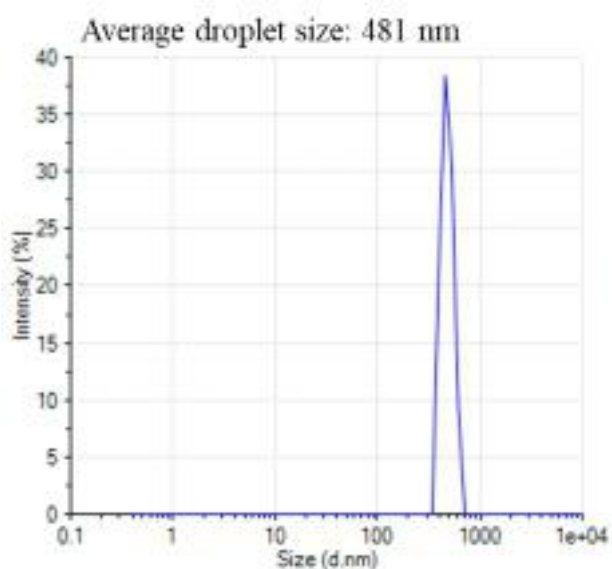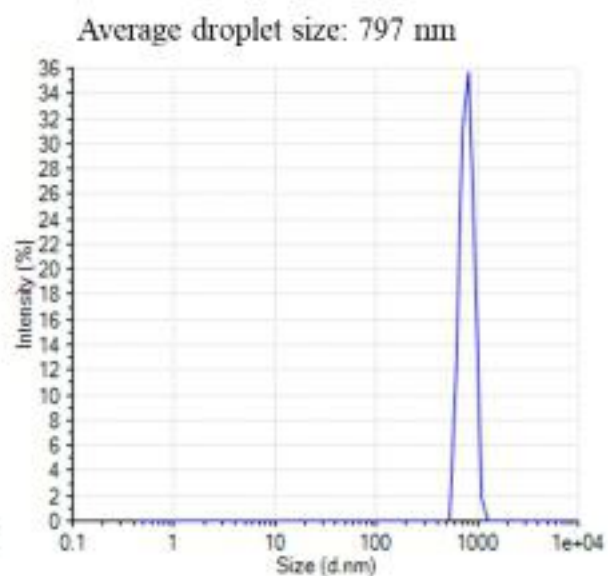
Average droplet size: 797 nm
(d)

626 **Figure S5.** Water droplet size distribution for water-in-oil emulsion with (a) 2.15 wt%, (b) 4.71

627 wt%, (c) 7.44 wt% and (d) 11.27 wt% water.
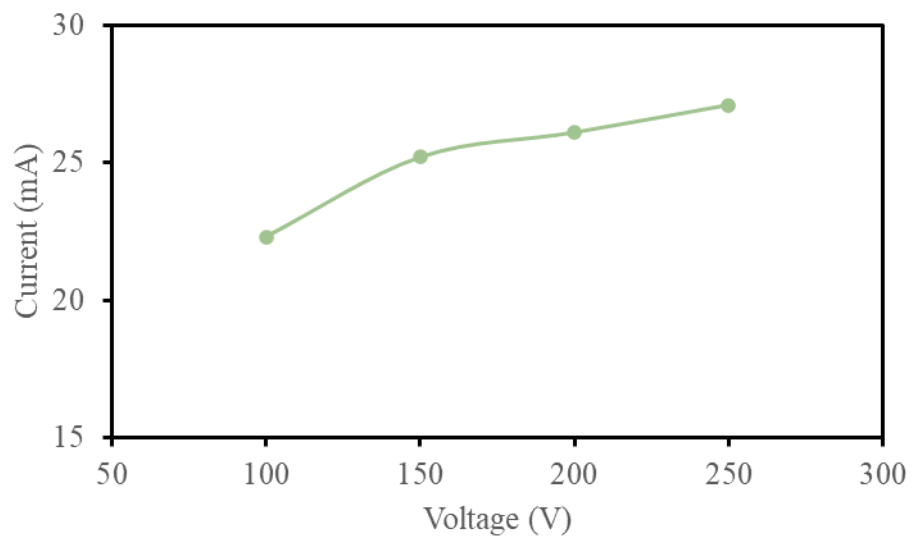
628

629 **Figure S6.** Current voltage characteristics of the system.

630